Primary osteosarcoma of the kidney: A case report

KUN ZHANG, LONGGUO DAI, HUIJIAN WAN, BINGYU ZHU, YANG WANG, ENFA NING, FEIYU YIN, JI LI, CHONGJINA ZHANG and YU BAI

Department of Urology, Yunnan Cancer Hospital, The Third Affiliated Hospital of Kunming Medical University, Kunming, Yunnan 650000, P.R. China

Received July 2, 2024; Accepted September 11, 2024

DOI: 10.3892/ol.2024.14732

Abstract. Primary renal osteosarcoma is an exceedingly rare subtype of renal malignancy, noted for its aggressive nature and often fatal outcome. The scarcity and severity of this condition have resulted in a dearth of reliable methods for early diagnosis and effective treatment. The present article contributes to the existing body of knowledge by presenting a comprehensive clinical case of a 46-year-old male patient with primary renal osteosarcoma. The detailed analysis of the clinical features, imaging characteristics, treatment approaches and prognosis of the patient in the present case aimed to enhance the understanding of renal osteosarcoma and inform clinical decision-making. The patient initially presented with painless hematuria, and further diagnostic work-up, including imaging and pathology, confirmed the diagnosis of primary renal osteosarcoma.

Introduction

Extraosseous osteosarcoma is an exceedingly rare soft-tissue malignancy, constituting <1% of all primary renal tumors (1,2). This form of primary renal osteosarcoma is highly malignant, and effective treatment strategies remain elusive. A review of historical case studies (3,4) revealed that patients with primary renal osteosarcoma often lack distinctive imaging and clinical features, which leads to many being diagnosed at an advanced stage with consequently poor treatment outcomes. Although a small subset of patients have been observed to be free of recurrence or metastasis for up to 68 months post-surgery, the majority are diagnosed at an advanced stage, with an average survival time of ~15 months (5). The present report describes the clinicopathological characteristics of a patient with primary renal osteosarcoma, offering new insights and potential reference points for the diagnosis and management of this rare condition.

Correspondence to: Professor Yu Bai, Department of Urology, Yunnan Cancer Hospital, The Third Affiliated Hospital of Kunming Medical University, 519 Kunzhou Road, Xishan, Kunming, Yunnan 650000, P.R. China
E-mail: baiyu@kmmu.edu.cn

Key words: extraskeletal osteosarcoma, primary osteosarcoma of the kidney, diagnosis

Case report

Case introduction. The patient, a 46-year-old male, presented with a 2-month history of hematuria without an identifiable trigger, and the symptoms had worsened over the month prior to admission. In April 2024, a CT examination was performed at Yuxi People's Hospital (Yuxi, China), revealing a mass-like tissue density in the lower middle portion of the left kidney, measuring ~7.7x6.4 cm. This finding was accompanied by evidence of cancerous thrombosis in the left renal vein and the presence of multiple enlarged retroperitoneal lymph nodes (data not shown). Consequently, the patient was directed to Yunnan Cancer Hospital (Kunming, China) for additional diagnostic procedures and treatment, with the referral taking place in May 2024. The patient had a history of hypertension and a smoking habit spanning >20 years. Furthermore, the patient was diagnosed with renal failure in 2016, underwent a right kidney transplant in 2017 and had been on long-term immunosuppressant therapy and regular hemodialysis since the procedure. There were no significant abnormalities identified in the family medical history. A physical examination in Yunnan Cancer Hospital revealed a palpable, fixed and large mass beneath the left rib cage.

Routine test results indicated moderate anemia, with a hemoglobin level of 90 g/l (reference range, 130-175 g/l). The patient had an abnormally elevated urinary leukocyte count of 429.5/μl (normal reference range, 0-25/μl) and a similarly abnormal urinary erythrocyte count of 723.2/μl (normal reference range, 0-12/μl). Alkaline phosphatase levels were in the normal range (53 U/l; reference range, 45-125 U/l). Tumor marker tests revealed the following: Carcinoembryonic antigen, 19.1 ng/ml (reference range, <5 ng/ml); carbohydrate antigen (CA) 19-9, 478.7 U/ml (reference range, 0-30 U/ml); and CA 242, 84.2 U/ml (reference range, 0-10 U/ml). The glomerular filtration rate for the left kidney was 5.15 ml/min (reference range, 90-120 ml/min), and for the right kidney it was 6.43 ml/min, with all other indicators within the normal range.

Further CT examination at Yunnan Cancer Hospital revealed a mass-shaped cystic focus beneath the cortex of the left kidney, measuring ~7.4x6.9x12.5 cm (Fig. 1). This focus showed scattered internal pneumatization, a hypodense filling

defect in the left renal vein and multiple enlarged retroperitoneal lymph nodes. The patient subsequently underwent surgical resection of the affected kidney, which measured 14x10x8 cm. Upon incision along the renal hilum, a grayish-red, solid mass measuring 8x6x5.5 cm was observed, along with several hilar lymph nodes with diameters ranging from 1.5-4 cm.

Pathological examination, following hematoxylin and eosin (H&E) staining, disclosed hyperplasia of short spindle cells accompanied by necrosis (Fig. 2A and B). Intravascular tumor thrombi tested positive, and metastatic involvement was identified in the renal hilar lymph nodes. However, no tumor invasion was detected in the renal pelvis or ureter upon dissection.

Immunohistochemical analysis demonstrated the following positive results: Vimentin, CD56, smooth muscle actin (SMA), special AT-rich sequence-binding protein 2 (SATB-2), P53, minimal weak positivity for GATA-Binding Factor 3 (GATA-3), scattered positivity for CK5/6, weak to positive expression of epithelial membrane antigen (EMA), partial positivity for actin, weak P504s, partially weak transcription factor E3 (TFE-3), minimal positivity for S-100. The expression rate of Ki67 was ~60%, and succinate dehydrogenase complex iron sulfur subunit B (SDHB) was also expressed in the tumor tissue. (Fig. 2C-F). Conversely, the analysis revealed negative results for CK8, paired box (Pax)-8, Pax-2, P63, human melanoma black 45 (HMB-45), CD34, Wilms tumor protein 1 (WT-1), E-cadherin, CK, CK7, Desmin, H-caldesmon, Myogenin, transcription termination factor 1 (TTF-1), P40, Calponin, CD10, CD117, Syn and chromogranin A (CgA) (data not shown).

Given the extreme rarity of the condition and the absence of osseous material in the tissue samples, diagnosis was highly challenging. Consequently, a pathological consultation was sought from the Ruijin Hospital Affiliated with Shanghai Jiao Tong University School of Medicine (Shanghai, China). The expert team at Ruijin Hospital conducted a comprehensive assessment of the patient, including microscopic examination, immunohistochemical analysis, and pathological evaluation, leading to the definitive diagnosis of primary renal osteosarcoma. The pathological staging was determined to be pT3aN1M0, in accordance with the 2017 American Joint Committee on Cancer staging for renal cancer (6). A total of 2 months after the surgical procedure, the patient returned to Yunnan Cancer Hospital for a follow-up examination. PET-CT disclosed irregular tissue density shadows with elevated metabolism in the surgical region (data not shown) and a maximum standardized uptake value (SUVmax) of 21. This finding was indicative of tumor recurrence. Additionally, the scan revealed multiple hypermetabolic nodules in several locations, including the left posterior renal space, the angle of the left diaphragm, the left paraspinal muscles, and the left lumbar psoas major muscles (data not shown). These were suggestive of tumor metastases. Moreover, PET-CT identified multiple hypermetabolic lymph nodes in the middle and lower retroperitoneum (data not shown with an SUVmax of 25.5, which were suggestive of tumor metastases. Considering the swift progression of the illness, the poor physical condition of the patient, and after a thorough review of the therapeutic options, the patient was started on a combination chemotherapy regimen that included cisplatin, adriamycin and cyclophosphamide. However, due to the poor physical condition of the patient, they were lost to follow-up after completing a cycle of chemotherapy.

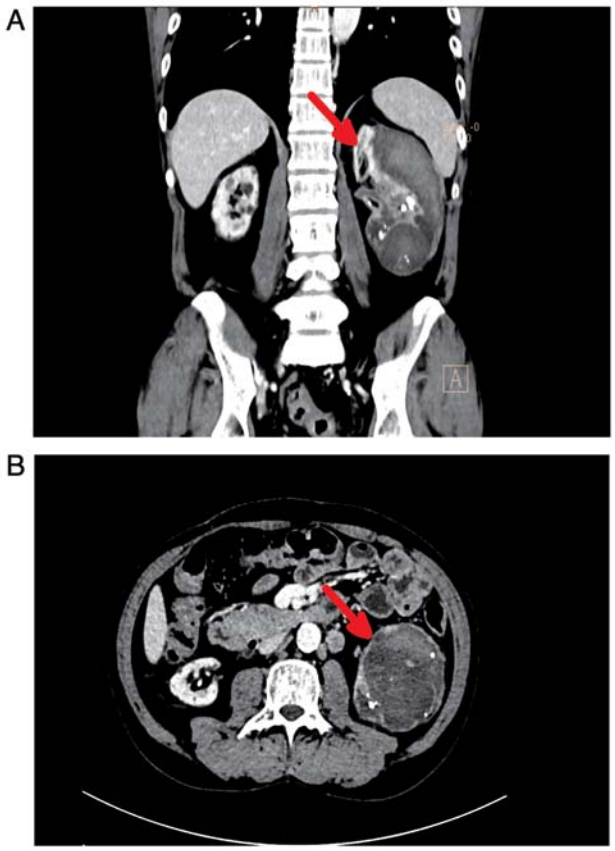

Figure 1. CT images. (A) Coronal and (B) axial planes demonstrate the mass as exhibiting mixed-density characteristics.

Methodology. For H&E staining, the tissue samples were fixed in 10% formalin for 24 h at room temperature, ensuring the preservation of tissue structure. The fixed tissues were then embedded in paraffin to facilitate the subsequent sectioning, yielding sections with a uniform thickness of 4-6 μm. The staining sequence involved an initial application of Gill II hematoxylin for 15 min at room temperature, providing a blue color to the cell nuclei, followed by a brief eosin staining for 30 sec at room temperature, which imparted a pink hue to the cytoplasm. Post-staining, the sections underwent a dehydration process to prepare for mounting. The dehydrated sections were mounted with neutral balsam, safeguarding the stained layer and enhancing sample stability. The mounted sections were then scrutinized under a light microscope to elucidate the cellular and tissue architecture.

For immunohistochemistry, the ready-to-use UltraSensitive™ SAP immunohistochemistry kit (cat. no. KIT-9710); Fuzhou Maixin Biotechnology Development Co., Ltd.) was used, and the procedure was as follows (all conditions are the same as H&E): Initially, the deparaffinization and hydration step was performed, where paraffin-embedded tissue sections were treated with xylene and a descending series of alcohol concentrations, followed by rinsing with tap water to remove paraffin from the sections and rehydrate the tissue. Subsequently, the primary antibodies were incubated overnight at 4˚C. All antibodies and staining reagents used were purchased from Fuzhou Maixin Biotechnology Development Co., Ltd. and were provided pre-diluted by the manufacturer: Vimentin (cat. no. MAB-0735),

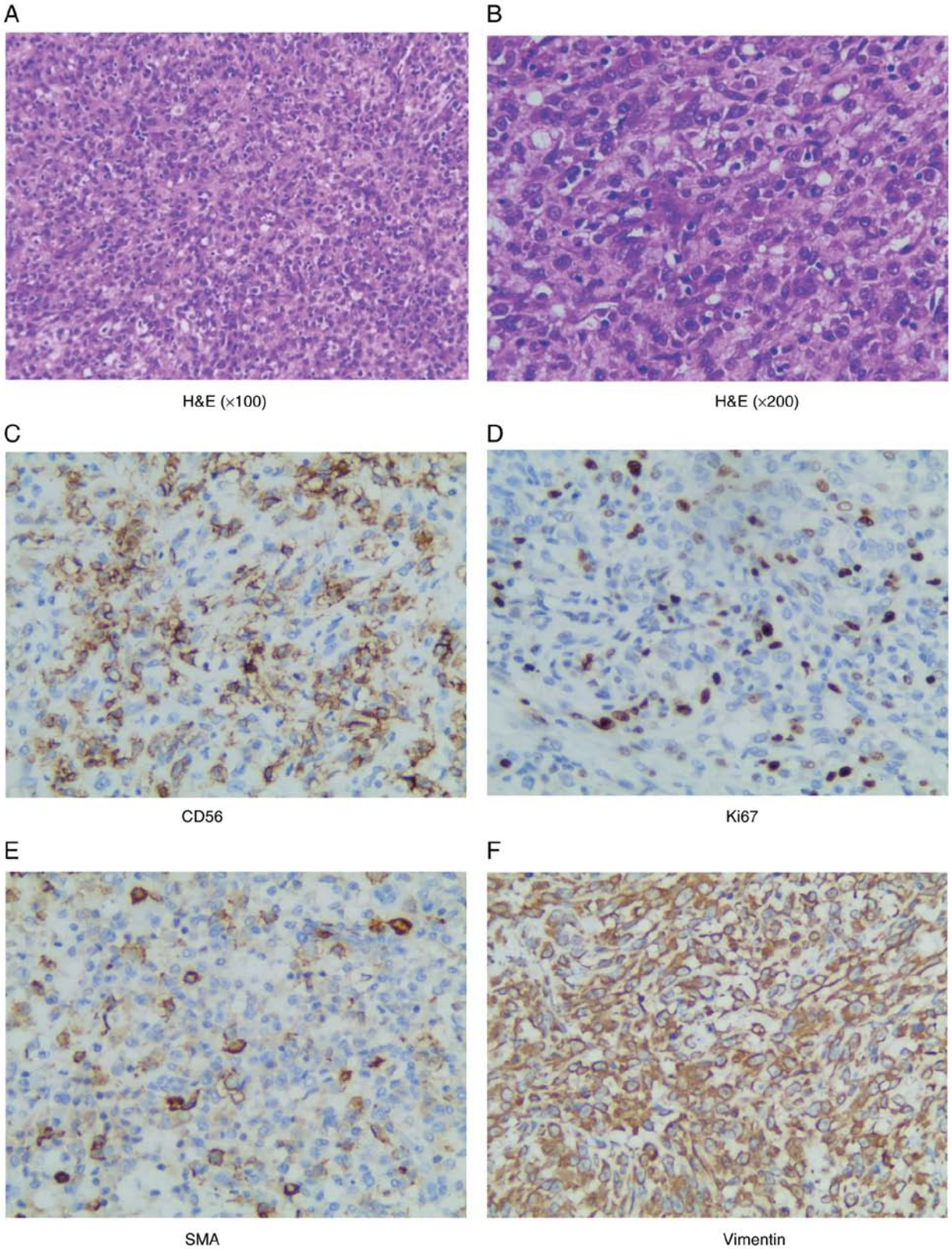

Figure 2. Histopathological and immunohistochemistry staining images showing the results of microscopic examination after H&E staining, which reveal extensive hyperplasia of short spindle-shaped cells interspersed with areas of necrosis. (A) H&E (magnification, x100), (B) H&E (magnification, x200), (C) CD56 positive (magnification, x200), (D) Ki67 positive (magnification, x200), (E) SMA positive (magnification, x200) and (F) Vimentin positive (magnification, x200). H&E, hematoxylin-eosin; SMA, smooth muscle actin.

CD56 (cat. no. MAB-0743), SMA (cat. no. MAB-0890), SATB-2 (cat. no. RMA-0750), P53 (cat. no. MAB-0674), GATA-3 (cat. no. MAB-0695), CK5/6 (cat. no. MAB-0744), EMA (cat. no. Kit-0011), actin (cat. no. MAB-0871), P504s (cat. no. RMA-0546), TFE-3 (cat. no. RMA-0663), S-100 (cat. no. RAB-0150) and Ki67 (cat. no. MAB-0672), SDHB

(cat. no. MAB-0888), CK8 (cat. no. MAB-1002), CK18 (cat. no. MAB-0737), Pax-8 (cat. no. MAB-0837), Pax-2 (cat. no. RMA-0816), P63 (cat. no. MAB-0694), HMB-45 (cat. no. MAB-0098), CD34 (cat. no. Kit-0004), WT-1 (cat. no. MAB-0678), E-cadherin (cat. no. MAB-0738), CK (cat. no. RAB-0050), CK7 (cat. no. MAB-0828), Desmin (cat. no. MAB-0766), H-caldesmon (cat. no. MAB-0634), Myogenin (cat. no. MAB-0866), TTF-1 (cat. no. MAB-0677), P40 (cat. no. RMA-0815), Calponin (cat. no. MAB-0712), CD10 (cat. no. MAB-0668), CD117 (cat. no. Kit-0029), Syn (cat. no. MAB-0742) and CgA (cat. no. RMA-0548). Following this, a peroxidase blocking step was performed to prevent interference from endogenous peroxidase activity. This involved the removal of PBS, application of the peroxidase blocking reagent, and a 10-min incubation at room temperature, after which the sections were rinsed three times with PBS for 3 min each. The non-specific staining blocking step was then implemented by applying a non-specific staining blocker, incubation at room temperature for 10 min to reduce background staining, and rinsing again with PBS. After the removal of the blocking agent, the aforementioned primary antibodies were applied and incubated at room temperature for 60 min, followed by three rinses with PBS for 3 min each to ensure specific binding of the antibodies to the target antigen. Once PBS was removed, biotinylated secondary antibodies were added and incubated at room temperature for 10 min, then rinsed with PBS. Streptavidin-anti-biotin peroxidase reagent was introduced to further amplify the signal, with a subsequent 10-min incubation at room temperature and three rinses with PBS. The color development process was terminated using tap water after rinsing with PBS, and then fresh DAB chromogen reagent was applied to visualize the specifically bound antibody complex. After color development, hematoxylin counterstaining for 1-2 min at room temperature was performed to enhance the contrast of the cell nuclei, followed by bluing with PBS. Finally, the sections were mounted with synthetic resin and examined under a light microscope.

Discussion

Among primary renal malignancies, clear cell renal cell carcinoma is the most common, whilst the renal osteosarcoma subtype is exceedingly rare and highly aggressive (4). Historical case reports indicate that >50% of the patients are diagnosed with stage T4 disease accompanied by lymph node metastasis at the time of initial presentation, and distant metastases are found in >80% of cases (3). The patient in the present report was diagnosed with stage pT3aN1M0.

The most common symptoms of renal osteosarcoma include lower back pain and a palpable presence of a mass in the lumbar region (3). In cases of advanced disease, hematuria often emerges as the primary symptom (3). CT is a highly valuable diagnostic tool for renal malignancies. Characteristic CT features of renal osteosarcoma encompass a large, mixed-density, cystic-solid mass with areas of calcification, observed in ~50% of the patients (7). Furthermore, CT is instrumental in ruling out sarcomas of osseous origin and in detecting lymph node and systemic metastases. It has been suggested that renal osteosarcoma may exhibit a distinctive 'sunburst' pattern on imaging (8). MRI findings for extraosseous osteosarcoma are less well characterized. On T1-weighted images, the signal intensity is similar to that of skeletal muscle, whereas on T2-weighted images, it appears isointense or hyperintense (7). PET-CT typically demonstrates a high metabolic signal, often with a central necrotic region that may show reduced metabolic activity. Additionally, extraosseous osteosarcoma tends to exhibit a narrower range of SUVmax values compared with its osseous counterpart (7).

A review of the existing literature on primary renal osteosarcoma indicates that diagnosis is primarily achieved through a process of exclusion and the use of immunohistochemical diagnostic methods. Initially, it is crucial to rule out the metastasis of osteosarcoma tissues from other regions, requiring whole-body CT or MRI (9). In the present case, the patient showed no evidence of metastasis from other sources in the CT examination. Secondly, differentiating between ossification in renal clear cell carcinoma (RCC) and primary renal osteosarcoma is essential, as the existing literature highlights. The probability of RCC ossification is extremely low, and primary renal osteosarcoma does not contain carcinoma (8-10). The distinct tissue origins of RCC and primary renal osteosarcoma result in different expressions of immunohistochemical markers, which are key for differentiation (for example, Vimentin, CD56, SMA and SATB-2 positivity) (1). As the present case was distinctive in that no discernible bone-like tissue was observed in the resected kidney or metastatic lymph nodes, a multitude of immunohistochemical markers were used to substantiate the diagnosis through exclusion, and a comprehensive array of neoplastic cells was identified, including nephroblasts, uroepithelial, neurogenic, rhabdomyosarcoma and melanin. However, the expression of Vimentin, CD56, SMA, and SATB-2 in the tumor cells ultimately led to the diagnosis of primary osteosarcoma of the kidney.

In addition, with the popularization of genetic testing and targeted therapy, there have been reports on the genetic testing of primary renal osteosarcoma. The genes with differences reported include: Phosphatidylinositol-4,5-bisphosphate 3-kinase catalytic subunit α (PIK3CA), CCCTC-binding factor (CTCF), Ras p21 protein activator 1 (RASA1), MutS Homolog 6 (MSH6), Fanconi anemia complementation group F (FANCF) and excision repair cross-complementing rodent repair deficiency complementation group 4 (ERCC4) (3,8). Certain studies have suggested that the aforementioned genes may lead to tumor progression and poor prognosis in other types of cancer, and they may enhance the tumor response to chemotherapy (11,12). However, their role in renal osteosarcoma is currently not well understood.

In summary, the diagnostic criteria for primary renal osteosarcoma are encapsulated by the following points: i) Imaging assessment: Renal space-occupying lesions are identified via CT or MRI, with meticulous exclusion of extra-renal metastases; ii) immunohistochemical profiling: Tumor cells are found to express osteoblast-differentiation markers, such as Vimentin, CD56, SMA and SATB-2; and iii) differentiation from other renal tumors: A definitive exclusion of alternative renal neoplasms, notably ossified renal cell carcinoma, is imperative. Furthermore, the diagnosis of renal osteosarcoma is bolstered when imaging studies rule out metastatic renal tumors, and pathological examination reveals the presence of bone-like components within the tumor.

The primary treatment for renal osteosarcoma is surgery, with the objective of achieving complete tumor resection and

ensuring negative surgical margins. Whilst there is a limited body of research on chemotherapeutic regimens specific to renal osteosarcoma, a study on extraosseous osteosarcoma indicated that platinum-based adjuvant chemotherapy can markedly extend patient survival (13). A commonly used treatment protocol involves a triple drug combination of doxorubicin, ifosfamide and cisplatin (9). A study also explored the potential of targeted therapy, particularly in conjunction with anlotinib (8). Radiotherapy is frequently used in the treatment of extraosseous osteosarcoma, with evidence suggesting it is more effective than chemotherapy for improving recurrence-free survival. Moreover, the concurrent use of radiotherapy and chemotherapy has been demonstrated to notably enhance patient survival rates compared with surgery alone (14,15). However, there is a scarcity of cases involving the use of radiotherapy for primary renal osteosarcoma. One documented case involved a patient who experienced local recurrence shortly after undergoing postoperative radiotherapy at a dose of 50 Gy and was then switched to adjuvant chemotherapy involving methotrexate and vincristine (4). After comprehensive consideration, the patient was given a combination chemotherapy regimen consisting of cisplatin, adriamycin and cyclophosphamide.

In conclusion, primary renal osteosarcoma is an exceedingly rare malignancy, with a mere 30 documented cases reported to date. Clinical symptoms of this condition are often subtle in the early stages, making them easily overlooked by patients. It is not uncommon for the disease to progress to later stages before symptoms such as lower back pain and hematuria become apparent. The present report describes a case where hematuria was the initial presenting symptom. Additionally, a comprehensive review of the imaging characteristics and therapeutic approaches from previous cases are discussed, with the intent of providing a reference that may aid in the early diagnosis and treatment of primary renal osteosarcoma.

Acknowledgements

Not applicable.

Funding

The present research was funded by the National Natural Science Foundation of China (grant no. 82160511) and the National Cancer Center Climbing Fund (grant no. NCC201925B01).

Availability of data and materials

The data generated in the present study may be requested from the corresponding author.

Authors' contributions

KZ, LD and HW designed the study and wrote the manuscript. BZ and YW advised on patient treatment, analyzed patient data and confirm the authenticity of all the raw data. KZ, LD and HW gathered medical pictures and assessed the patient information. EN, FY, JL, CZ and YB contributed to the conceptualization of the study, general design and quality assurance. All authors have read and approved the final manuscript.

Ethics approval and consent to participate

Not applicable.

Patient consent for publication

The patient provided informed consent for publication of the present case report and associated images.

Competing interests

The authors declare that they have no competing interests.

References

1. Ahomadégbé C, Bennani-Guebessi N and Karkouri M: Primary renal osteosarcoma: A case report. Afr J Urol 20: 189-192, 2014.
2. Uhlig J, Uhlig A, Bachanek S, Onur MR, Kinner S, Geisel D, Köhler M, Preibsch H, Puesken M, Schramm D, *et al*: Primary renal sarcomas: Imaging features and discrimination from non-sarcoma renal tumors. Eur Radiol 32: 981-989, 2022.
3. Chen J, Liao H, Zhan R, Zheng Q, Deng J, Wang G and Zhang J: Case report: Primary osteosarcoma of the kidney. Front Oncol 13: 1175518, 2023.
4. Weingärtner K, Gerharz EW, Neumann K, Pflüger KH, Grüber M and Riedmiller H: Primary osteosarcoma of the kidney. Case report and review of literature. Eur Urol 28: 81-84, 1995.
5. Lopez-Beltran A, Montironi R, Carazo JL, Vidal A and Cheng L: Primary renal osteosarcoma. Am J Clin Pathol 141: 747-752, 2014.
6. Paner GP, Stadler WM, Hansel DE, Montironi R, Lin DW and Amin MB: Updates in the eighth edition of the tumor-node-metastasis staging classification for urologic cancers. Eur Urol 73: 560-569, 2018.
7. Hesni S, Lindsay D, O'Donnell P and Saifuddin A: Extra-skeletal osteosarcoma: A review. Skeletal Radiol 52: 633-648, 2023.
8. Huang C, Zhu X, Xiong W, Zhao X and Xu R: A case report of primary osteosarcoma originating from kidney. Medicine (Baltimore) 98: e14234, 2019.
9. Allan CJ and Soule EH: Osteogenic sarcoma of the somatic soft tissues. Clinicopathologic study of 26 cases and review of literature. Cancer 27: 1121-1133, 1971.
10. Pan H, Wu D, Wang H, Pan Y, Zhang T and Zhou J: Clear cell renal cell carcinoma with extensive osseous metaplasia: Report of a rare case. Urology 105: e3-e5, 2017.
11. Wang MJ, Zhu Y, Guo XJ and Tian ZZ: Genetic variability of genes involved in DNA repair influence treatment outcome in osteosarcoma. Genet Mol Res 14: 11652-11657, 2015.
12. Zehir A, Benayed R, Shah RH, Syed A, Middha S, Kim HR, Srinivasan P, Gao J, Chakravarty D, Devlin SM, *et al*: Mutational landscape of metastatic cancer revealed from prospective clinical sequencing of 10,000 patients. Nat Med 23: 703-713, 2017.
13. Paludo J, Fritchie K, Haddox CL, Rose PS, Arndt CAS, Marks RS, Galanis E, Okuno SH and Robinson SI: Extraskeletal osteosarcoma: Outcomes and the role of chemotherapy. Am J Clin Oncol 41: 832-837, 2018.
14. Heng M, Gupta A, Chung PW, Healey JH, Vaynrub M, Rose PS, Houdek MT, Lin PP, Bishop AJ, Hornicek FJ, *et al*: The role of chemotherapy and radiotherapy in localized extraskeletal osteosarcoma. Eur J Cancer 125: 130-141, 2020.
15. Campos F, Téres R, Sebio A, Bettim BB and Martinez-Trufero J: Survival differences of patients with resected extraskeletal osteosarcoma receiving two different (Neo)adjuvant chemotherapy regimens: A systematic review and meta-analysis. Clin Oncol (R Coll Radiol) 35: e720-e727, 2023.